Journal of the Ceramic Society of Japan 117 [4] 426-430 2009 **Paper**

Epitaxial growth of $BaRuO_3$ thin films on MgO substrates by laser ablation

Akihiko ITO†, Hiroshi MASUMOTO,* Takashi GOTO and Shunichi SATO**

Institute of Multidisciplinary Research for Advanced Materials, Tohoku University, Sendai 980−8577
***Center for Interdisciplinary Research, Tohoku University, Sendai 980−8578**
****Institute for Materials Research, Tohoku University, Sendai 980−8577**

Epitaxial $BaRuO_3$ (BRO) thin films were prepared on (001) and (111) MgO substrates by laser ablation, and the relationship of lattice matching, morphology and electrical conductivity was investigated. (205)- and (001)-oriented rhombohedral BRO thin films were epitaxially grown on (001) and (111) MgO substrates, respectively. The (205) BRO thin films showed an orthogonal texture with faceted island grains, whereas the (001) BRO thin films had a hexagonal columnar structure with a flat terrace. Epitaxial BRO thin films showed metallic conduction, and the (205) BRO thin films exhibited the highest electrical conductivity, *i.e.*, 1.0×10^5 S·m^{-1}, at room temperature. A higher lattice matching between epitaxial thin film and the substrate yielded a higher electrical conductivity.

Key-words : Laser ablation, Barium ruthenate, Thin films, Epitaxial growth, Microstructure, Electrical conductivity

[Received November 10, 2008; Accepted January 15, 2009]

1. Introduction

Ruthenium-based oxides $ARuO_3$ (A = Ca, Sr and Ba) are potential candidates for electrode material of micro-devices because of their excellent electrical conductivity and fatigue properties.[1),2)] Although $CaRuO_3$ (CRO) and $SrRuO_3$ (SRO) are constructed from only corner-sharing RuO_6 octahedra,[3)] $BaRuO_3$ (BRO) exhibits polytypes depending on the numbers of periodically stacked corner- and face-sharing RuO_6 octahedra, such as 9R ($R\bar{3}m$: a = 0.575 nm, c = 2.161 nm),[4),5)] 4H ($P6_3/mmc$: a = 0.574, c = 0.950 nm)[6)] and 6H ($P6_3/mmc$: a = 0.574, c = 1.405 nm),[7)] and exhibits characteristic electrical properties different from those of CRO and SRO due to the small Ru-Ru distance in the face-sharing RuO_6 octahedra.[8)]

Many studies on BRO thin films grown on the single-crystal substrates such as $SrTiO_3$ (STO),[9)–12)] $LaAlO_3$ (LAO)[13)] and Si[14),15)] have been conducted; however, study on the morphology and electrical properties of thin films epitaxially grown on a slightly mismatched substrate would help to clarify the mechanism of epitaxial growth. Moreover, since MgO ($Fm\bar{3}m$: a = 0.422 nm) is an inexpensive and accessible material, it would be a favorable substrate for practical usage.

In this study, BRO thin films were prepared on (001) and (111) MgO substrates, and the relationship between lattice matching, morphology and electrical conductivity was investigated.

2. Experimental procedure

$BaCO_3$ (99.9% purity, Wako Pure Chemical Industries, Ltd.) and RuO_2 (99.99% purity, Furuya Metal Co., Ltd.) powders were used for preparation of laser ablation targets. These powders were weighed, mixed, pressed into pellets and reacted at 1273 K for 36.0 ks to obtain BRO pellets. These pellets were crushed and sintered again at 1573 K for 43.2 ks, and thus the BRO targets were obtained.

A third harmonic wavelength (λ = 355 nm) of a Q-switch pulsed Nd:YAG was used for the ablation. The details of the experimental procedure have been reported elsewhere.[16)] The deposition was carried out in O_2 at a pressure (P_{O_2}) of 13 Pa and a substrate temperature (T_{sub}) of 973 K. (001) and (111) MgO single-crystal plates (10 × 10 × 0.5 mm) were used as substrates. Thin films of approximately 100 nm in thickness were obtained by laser ablation for 3.6 ks.

The crystal phase was studied by X-ray diffraction (XRD, Rigaku RAD–2C). The in-plane orientation of film was determined by using pole figure X-ray diffraction (Rigaku RAD–C). The thickness was measured by a profilometer (Taylor–Hobson Talystep). Film growth during the deposition was monitored using *in situ* reflection high-energy electron diffraction (RHEED). The surface morphology was observed by field-emission scanning electron microscopy (FESEM, JEOL JSM–6500FT). The electrical conductivity was measured by the van der Pauw method from 60 to 693 K.

3. Results and discussion

Figure 1 shows the XRD patterns of the BRO thin films prepared on (001) and (111) MgO substrates at P_{O_2} = 13 Pa and T_{sub} = 973 K. (205)-oriented 9R BRO thin films were grown epitaxially on (001) MgO substrates with a minor amount of (001) and (024) 9R BRO orientation phases (Fig. 1(a)). In this paper, the crystal planes of rhombohedral BRO are indexed as hexagonal notations. On the (111) MgO substrates, although small peaks from (104), (024) and (205) 9R BRO planes were observed, BRO thin films were significantly oriented to the (001) 9R BRO plane (Fig. 1(b)).

Figure 2 depicts the pole figure X-ray diffraction patterns of the epitaxial BRO thin films prepared on (001) and (111) MgO substrates. The pole figure patterns for the MgO substrates are depicted in the same figures. Four reflections from (001) BRO planes of the BRO thin film were obtained in the pole figure of

† Corresponding author: A. Ito; E-mail: itonium@tagen.tohoku.ac.jp

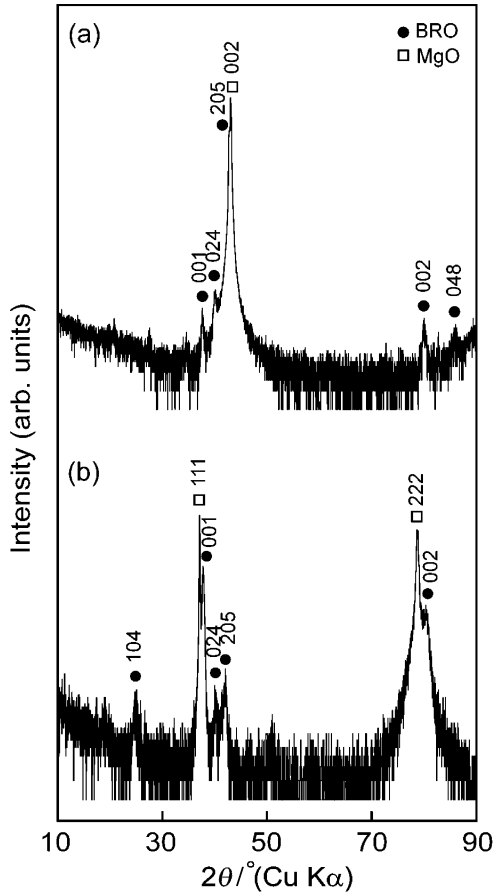

Fig. 1. XRD patterns of BRO thin films prepared on (001) MgO (a) and (111) MgO (b) substrates.

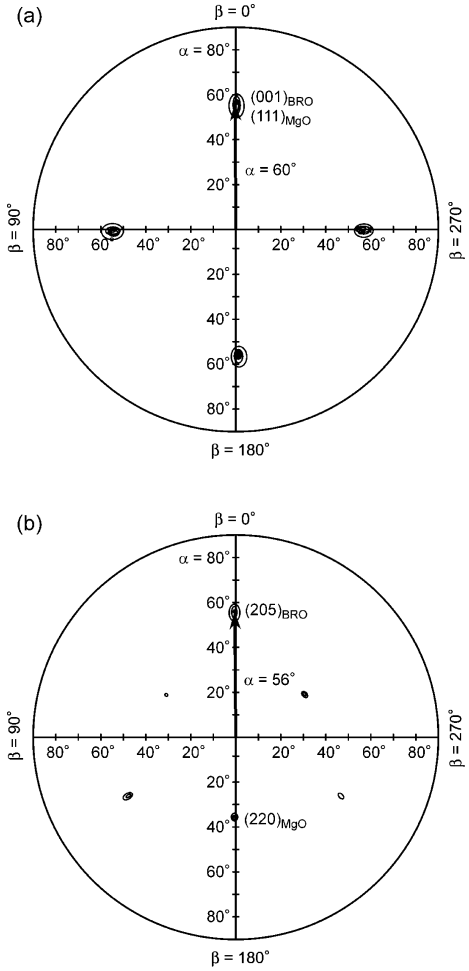

Fig. 2. X-ray pole figures of BRO thin films prepared on (001) MgO (a) and (111) MgO (b) substrates.

the BRO thin film grown on (001) MgO substrate at $\alpha = 60°$ (Fig. 2(a)), and three reflections from (205) BRO planes were obtained in the pole figure of the (001) BRO thin film grown on (111) MgO substrate at $\alpha = 56°$ (Fig. 2(b)). It can be therefore concluded that BRO thin films were epitaxially oriented to the MgO substrates. The in-plane epitaxial relationship can be summarized as follows: [010] BRO // [110] MgO with (205) BRO/(001) MgO, and [110] BRO // [$\bar{1}\bar{1}$2] MgO with (001) BRO/(111) MgO.

Figure 3 shows *in situ* RHEED patterns of epitaxial BRO thin films prepared on (001) and (111) MgO substrates. It is generally known that a streak reflection pattern in RHEED can be obtained from a step-and-terrace texture, whereas a spot transmission pattern can be obtained from an island texture.[17] The (205) BRO thin films prepared on (001) MgO substrates showed a spot pattern, implying that BRO island grains should grow on the MgO substrate (Fig. 3(a)), whereas the streak pattern of (001) BRO thin film implies a terraced texture (Fig. 3(b)). The Debye–Scherrer rings observed in RHEED patterns suggest an orientation fluctuation at the near-surface region of epitaxial thin films.

Figure 4 shows the surface morphology of BRO thin films prepared on (001) and (111) MgO substrates. The (205) BRO thin films showed an orthogonal texture with faceted island grains (Figs. 4(a), (b)). These faceted grains had a tetragonal or hexagonal shape, and tetragonal facets composed the orthogonal texture. The (001) BRO thin films had a hexagonal columnar texture with flat terraces (Figs. 4(c), (d)). This hexagonal structure may be reflected in the crystallographic feature of the (001) BRO plane. These island and terraced textures, respectively, well

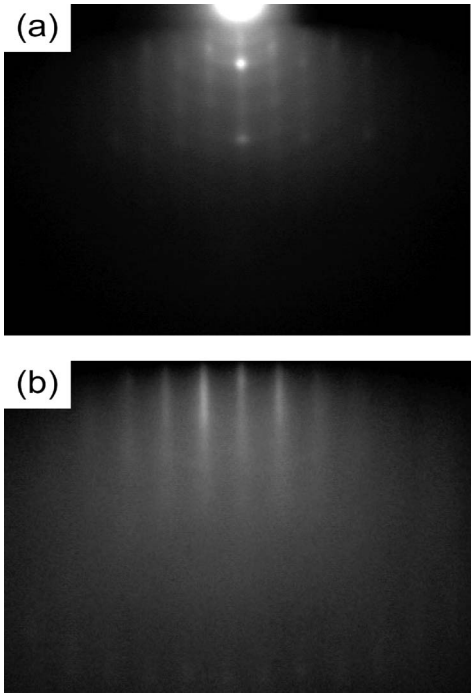

Fig. 3. *in situ* RHEED diffraction patterns of BRO thin films prepared on (001) MgO (a) and (111) MgO (b) substrates.

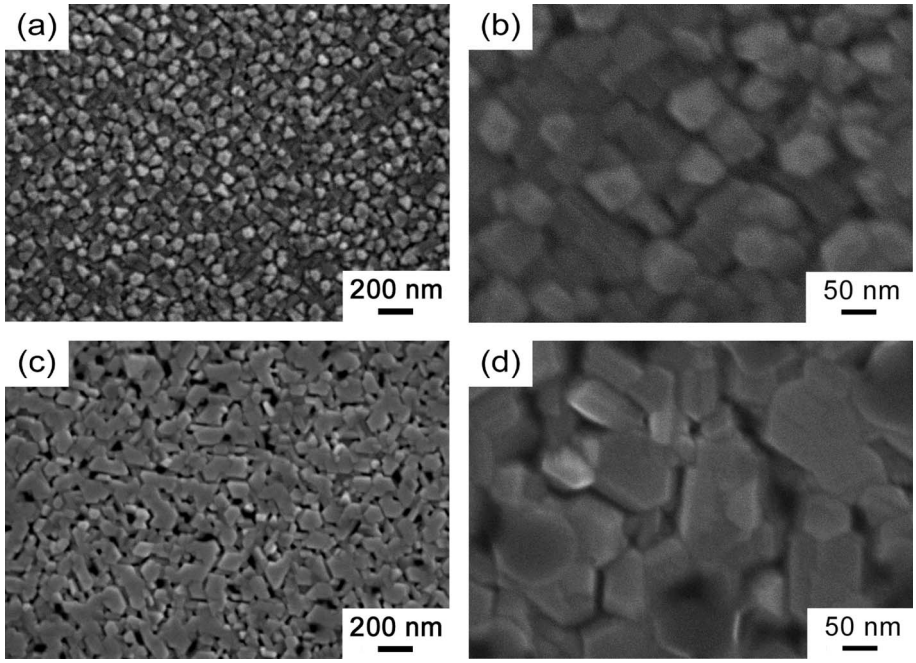

Fig. 4. Low and high magnification FESEM images of BRO thin films prepared on (001) MgO (a, b) and (111) MgO (c, d) substrates, respectively.

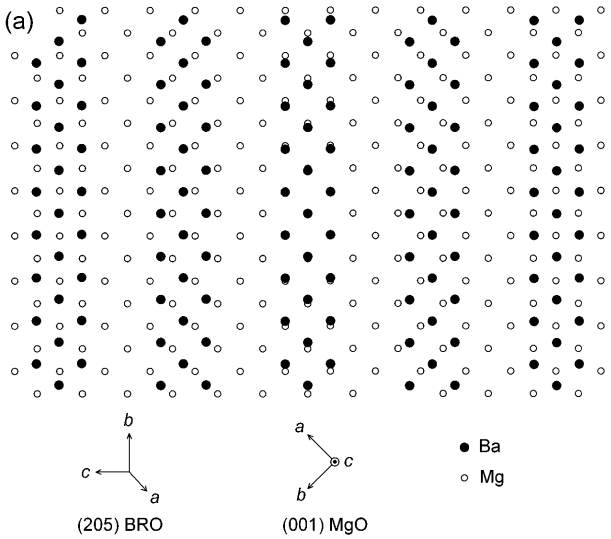

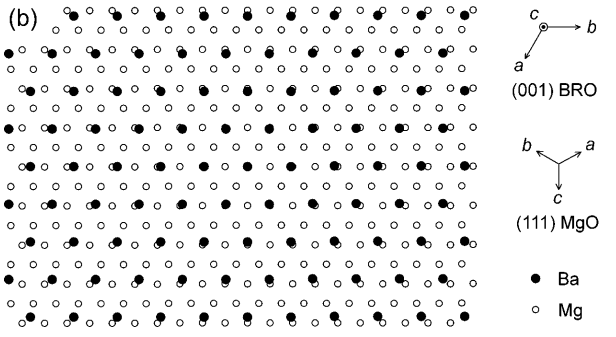

Fig. 5. Schematic plan-view of (205) BRO plane on (001) MgO (a) and (001) BRO plane on (111) MgO (b). Only Ba and Mg atoms are described for the sake of simplicity.

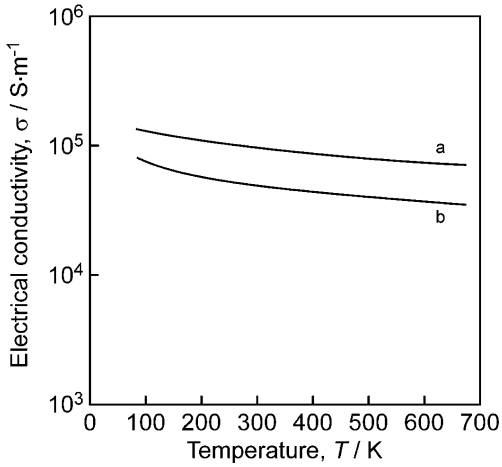

Fig. 6. Temperature dependence of electrical conductivity of BRO thin films prepared on (001) MgO (a) and (111) MgO (b) substrates.

corresponded to the spotty and streaky RHEED patterns shown in Fig. 3.

Figure 5 illustrates a schematic plan-view of the (205) BRO plane on (001) MgO plane and that of the (001) BRO plane on (111) MgO plane. For the sake of simplicity, only Ba and Mg atoms are described. (205) BRO plane has a slightly distorted tetragonal lattice of Ba atoms with the interior angles of 87.6 and 92.4°, and the atomic distance of Ba and Mg atoms along the [100] MgO direction are a_{Ba} = 0.415 nm and a_{Mg} = 0.422 nm, respectively (Fig. 5(a)). This atomic arrangement indicates that the BRO thin film can be oriented to the (205) plane on the (001) MgO substrates. Epitaxial (205) BRO thin films have also been obtained on the cubic lattice of (001) STO and (001) LAO substrates.[11),13),18),19)] The crystallographic feature of (205) BRO thin films can be observed as an orthogonal texture, as shown in

Table 1. Literature Data on the Orientation, Morphology and Electrical Conductivity of Epitaxial BRO thin Films Prepared on Various Single Crystal Substrates

Methods	Substrate	Orientation	Morphology	Conductivity [$\times 10^5$ S·m^{-1}]	Ref.
On (001) plane					
PLD	(001) STO	(205) 9R	–	1.0	11)
Sputtering	(001) STO	(02$\bar{2}$3) 4H	Orthogonal texture	1.0	10)
PLD	(001) STO	(205) (104) 9R	Orthogonal texture	0.8	18)
PLD	(001) LAO	(205) 9R	Orthogonal texture	7.1	13)
PLD	(001) LAO	(205) 9R	Orthogonal texture	0.7	19)
PLD	(001) MgO	(205) 9R	Ortho. texture with islands	1.0	Present study
On (111) plane					
Sputtering	(111) STO	(001) 4H	–	1.7	12)
Sputtering	(111) STO	(001) 4H	Concentric terraces	1.2	9)
PLD	(111) STO	(001) 9R	Hexagonal terraces	1.0	18)
PLD	(111) MgO	(001) 9R	Hexagonal columnar	0.5	Present study

PLD: pulsed laser deposition (laser ablation).

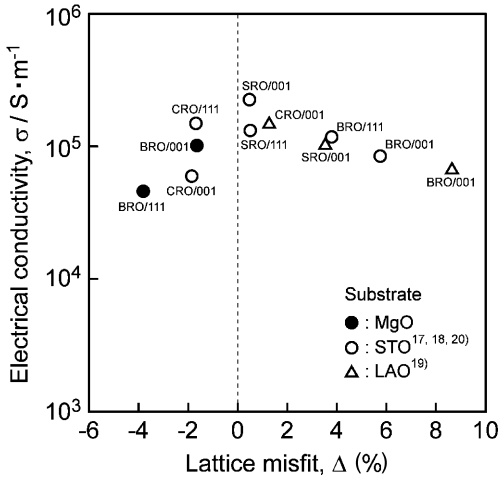

Fig. 7. Effect of lattice misfit on electrical conductivity of epitaxial BRO, CRO and SRO thin films prepared on (001) and (111) MgO (filled circles), (001) and (111) STO (open circles), and (001) LAO substrates (open triangles).

Figs. 4(a) and (b). On the other hand, the doubled atomic distance between Mg atoms of the (111) MgO plane ($2a_{Mg}$ = 0.596 nm) was nearly equal to the distance between Ba atoms of the (001) BRO plane (a_{Ba} = 0.575 nm). The triangular lattice of (111) MgO and (001) BRO plane produced a hexagonal terraced texture of the (001) BRO thin films, as shown in Figs. 4(c) and (d).

Figure 6 depicts the temperature dependence of electrical conductivity (σ) for BRO thin films prepared on (001) and (111) MgO substrates. Epitaxial BRO thin films showed metallic conduction, and the (205) BRO thin films prepared on (001) MgO substrates exhibited the highest electrical conductivity, *i.e.*, 1.0×10^5 S·m^{-1}, at room temperature. The decrease of σ for (001) BRO thin films could be understood as resulting from the gaps between hexagonal columnar grains.

Table 1 summarizes the literature data on the orientation, surface morphology and electrical conductivity of epitaxial BRO thin films prepared on various substrates.[9–13),18),19)] The BRO thin films prepared on the MgO substrates were similar in orientations and surface morphologies to those prepared on the STO and LAO substrates. BRO thin films prepared on (001) STO and (001) LAO substrates tended to grow with the (205) orientation, and had an orthogonal texture. On the (111) STO substrates, BRO thin films showed a hexagonal terraced texture, which grew along the *c*-axis of their hexagonal crystal structure. The BRO thin films prepared on STO substrates exhibited denser and smoother surfaces than those of the BRO thin films prepared on MgO substrates because of better lattice matching of BRO epitaxial planes to STO planes than to those of MgO.

Figure 7 shows the effect of the in-plane lattice misfit (Δ) between the epitaxial BRO thin films and MgO substrates on the σ at room temperature (filled circles). Open circles indicate the σ of epitaxial BRO,[18)] CRO[20)] and SRO[17)] thin films prepared on STO substrates by the present authors, and open triangles indicate such values for LAO substrates.[19)] The Δ can be calculated from eq. (1):

$$\Delta = (a_{film} - a_{sub})/a_{sub} \times 100, \quad (1)$$

where a_{film} and a_{sub} are, respectively, the distance between atoms in thin films (Ba, Ca and Sr) and that in substrates (Mg, Sr and La). The morphology and σ may be associated with the lattice matching between the thin films and substrates. A flat surface with a terrace-and-step structure was obtained at a Δ ranging from 0 to 2%, whereas the island texture grew at a Δ larger than 5%. In the case of Δ below 0%, the thin films tended to have an island structure with gaps between grains. The σ increased as the Δ came close to 0%.

4. Conclusions

Rhombohedral (205) and (001) BRO thin films were epitaxially grown on (001) and (111) MgO substrates, respectively, with in-plain orientation relationships. The (205) BRO thin films showed an orthogonal texture with faceted island grains, whereas the (001) BRO thin films had a hexagonal columnar texture with flat terraces. Epitaxial BRO thin films showed metallic conduction, and the (205) BRO thin films prepared on (001) MgO substrates exhibited the highest electrical conductivity, *i.e.*, 1.0×10^5 S·m^{-1}, at room temperature. The epitaxial thin film with the smooth surface may have been derived from the high lattice matching, thus exhibiting higher electrical conductivity.

Acknowledgements This research was supported in part by the Global COE Program of the Materials Integration International Center of Education and Research, Tohoku University, and by the Asian CORE Program, JSPS. This research was financially supported in part by Furuya Metal Co., Ltd. and Lonmin Plc. The authors are also grateful to the Japan Society of Powder and Powder Metallurgy for its financial support.

References

1) C. B. Eom, R. J. Cava, R. M. Fleming, J. M. Phillips, R. B. van Dover, J. H. Marshall, J. W. P. Hsu, J. J. Krajewski and W. F. Peck Jr, *Science*, **258**, 1766–1769 (1992).
2) T. Morimoto, O. Hidaka, K. Yamakawa, O. Arisumi, H. Kanaya, T. Iwamoto, Y. Kumura, I. Kunishima and S. Tanaka, *Jpn. J. Appl. Phys*., **39**, 2110–2213 (2000).
3) R. J. Bouchard and J. L. Gillson, *Mater. Res. Bull.*, **7**, 873–878 (1972).
4) J. J. Randall and R. Ward, *J. Am. Chem. Soc.*, **81**, 2629–2631 (1959).
5) P. C. Donohue, L. Katz and R. Ward, *Inorg. Chem.*, **4**, 306–310 (1965).
6) S.-T. Hong and A. W. Sleight, *J. Solid State Chem.*, **128**, 251–255 (1997).
7) J. M. Longo and J. A. Kafalas, *Mater. Res. Bull.*, **3**, 687–692 (1968).
8) Y. S. Lee, J. S. Lee, K. W. Kim, T. W. Noh, J. Yu, Y. Bang, M. K. Lee and C. B. Eom, *Phys. Rev. B*, **64**, 165109 (2001).
9) M. K. Lee, C. B. Eom, W. Tian, X. Q. Pan, M. C. Smoak, F. Tsui and J. J. Krajewski, *Appl. Phys. Lett.*, **77**, 364–366 (2000).
10) M. K. Lee, C. B. Eom, J. Lettieri, I. W. Scrymgeour, D. G. Schlom, W. Tian, X. Q. Pan, P. A. Ryan and F. Tsui, *Appl. Phys. Lett.*, **78**, 329–331 (2001).
11) J. Lettieri, I. W. Scrymgeour, D. G. Schlom, M. K. Lee and C. B. Eom, *Appl. Phys. Lett.*, **77**, 600–601 (2000).
12) Y. S. Lee, J. S. Lee, K. W. Kim, T. W. Noh, J. Yu, Y. Bang, M. K. Lee and C. B. Eom, *Phys. Rev. B*, **64**, 165109 (2001).
13) D. Kaur and K. V. Rao, *Solid State Comm.*, **128**, 391–395 (2003).
14) G. Mei, X. W-ping, Z. Lirong, L. Chenglu and C. Zechum, *Thin Solid Films*, **288**, 95–98 (1996).
15) J. H. Lee, P. Lin, J. C. Ho and C. C. Lee, *Electrochem. Solid-State Lett.*, **9**, G292–G295 (2006).
16) A. Ito, H. Masumoto and T. Goto, *Mater. Trans.*, **47**, 2808–2814 (2006).
17) A. Ito, H. Masumoto and T. Goto, *Mater. Trans.*, **48**, 227–233 (2007).
18) A. Ito, H. Masumoto and T. Goto, *Mater. Trans.*, **48**, 1919–1923 (2007).
19) A. Ito, H. Masumoto and T. Goto, *Thin Solid Films* (2009), doi: 10.1016/j.tsf.2009.02.021.
20) A. Ito, H. Masumoto and T. Goto, *J. Ceram. Soc. Japan*, **115**, 683–687 (2007).